NANO LETTERS

Letter

pubs.acs.org/NanoLett

Docetaxel-Loaded PLGA Nanoparticles Improve Efficacy in Taxane-Resistant Triple-Negative Breast Cancer

Charles J. Bowerman,[†,∥] James D. Byrne,[∥,§] Kevin S. Chu,[§] Allison N. Schorzman,[∥,Δ] Amanda W. Keeler,[Δ] Candice A. Sherwood,[Δ] Jillian L. Perry,[∥] James C. Luft,[∥,§] David B. Darr,[∥] Allison M. Deal,[&] Mary E. Napier,[○] William C. Zamboni,[∥,Δ,‡] Norman E. Sharpless,[∥,¶,#] Charles M. Perou,[∥,¶,⊥] and Joseph M. DeSimone*[,†,∥,§,‡,◆,□]

[†]Department of Chemistry, University of North Carolina at Chapel Hill, Chapel Hill, North Carolina 27515, United States

[∥]Lineberger Comprehensive Cancer Center, University of North Carolina at Chapel Hill, Chapel Hill, North Carolina 27599, United States

[§]Division of Molecular Pharmaceutics, Eshelman School of Pharmacy, University of North Carolina at Chapel Hill, Chapel Hill, North Carolina 27599, United States

[Δ]Division of Pharmacotherapy and Experimental Therapeutics, Eshelman School of Pharmacy, University of North Carolina at Chapel Hill, Chapel Hill, North Carolina 27599, United States

[&]Lineberger Comprehensive Cancer Center Biostatistics and Clinical Data Management Core, University of North Carolina at Chapel Hill, Chapel Hill, North Carolina 27599, United States

[○]HIV Cure Center, University of North Carolina at Chapel Hill, Chapel Hill, North Carolina 27599, United States

[‡]Carolina Center of Cancer Nanotechnology Excellence, University of North Carolina at Chapel Hill, Chapel Hill, North Carolina 27599, United States

[¶]Department of Genetics, University of North Carolina at Chapel Hill, Chapel Hill, North Carolina 27599, United States

[#]Division of Hematology/Oncology, Department of Medicine, University of North Carolina at Chapel Hill, Chapel Hill, North Carolina 27599, United States

[⊥]Department of Pathology and Laboratory Medicine, University of North Carolina at Chapel Hill, Chapel Hill, North Carolina 27599, United States

[◆]Department of Pharmacology, Eshelman School of Pharmacy, University of North Carolina at Chapel Hill, Chapel Hill, North Carolina 27599, United States

[□]Department of Chemical and Biomolecular Engineering, North Carolina State University, Chapel Hill, North Carolina 27607, United States

ABSTRACT: Novel treatment strategies, including nanomedicine, are needed for improving management of triple-negative breast cancer. Patients with triple-negative breast cancer, when considered as a group, have a worse outcome after chemotherapy than patients with breast cancers of other subtypes, a finding that reflects the intrinsically adverse prognosis associated with the disease. The aim of this study was to improve the efficacy of docetaxel by incorporation into a novel nanoparticle platform for the treatment of taxane-resistant triple-negative breast cancer. Rod-shaped nanoparticles encapsulating docetaxel were fabricated using an imprint lithography based technique referred to as Particle Replication in Nonwetting Templates (PRINT). These rod-shaped PLGA-docetaxel nanoparticles were tested in the C3(1)-T-antigen (C3Tag) genetically engineered mouse model (GEMM) of breast cancer that represents the basal-like subtype of triple-negative breast cancer and is resistant to therapeutics from the taxane family. This GEMM recapitulates the genetics of the human disease and is reflective of patient outcome and, therefore, better represents the clinical impact of new therapeutics. Pharmacokinetic analysis showed that delivery of these PLGA-docetaxel nanoparticles increased docetaxel circulation time and provided similar docetaxel exposure to tumor compared to the clinical

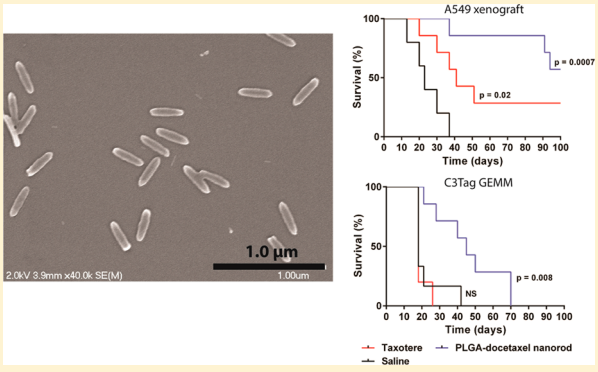

continued...

Received: September 22, 2016
Revised: December 3, 2016
Published: December 14, 2016

DOI: 10.1021/acs.nanolett.6b03971
Nano Lett. XXXX, XXX, XXX−XXX

formulation of docetaxel, Taxotere. These PLGA-docetaxel nanoparticles improved tumor growth inhibition and significantly increased median survival time. This study demonstrates the potential of nanotechnology to improve the therapeutic index of chemotherapies and rescue therapeutic efficacy to treat nonresponsive cancers.

KEYWORDS: *Nanoparticles, docetaxel, triple-negative breast cancer, genetically engineered mouse model, chemoresistance*

Nanomedicine has the potential to shift the paradigm for the delivery of cytotoxic agents. The lack of target specificity and unintended toxicities of conventional small molecule chemotherapies compromise the utility of this therapy as well as the patients' quality of life.[1] Nanoparticles are designed to alter the pharmacokinetic profiles and biodistribution of small molecule drugs or contrast agents in patients and enable the delivery of larger doses to the intended diseased tissue in an effort to improve therapeutic index, reduce systemic toxicity, and/or offer better imaging signals.[2,3] Currently, there are a number of clinically available nanomedicines, including Abraxane and Doxil, and others in clinical trials that have been shown to improve treatments for a variety of cancers.[1,4]

A key challenge to successful clinical translation of more nanomedicines for anticancer therapy has been defining the optimal physicochemical parameters that simultaneously confer molecular targeting, immune evasion, and controlled drug release.[5] Understanding the complex interdependence of these nanoparticle parameters is particularly important for improving delivery efficiency to tumors.[2] Using PRINT, we have previously explored the impact of size, shape, surface chemistry, and composition to achieve maximal tumor uptake.[6−12] These major particle parameters have been optimized for passive tumor targeting in subcutaneous models of cancer.[13−17]

Patients with triple-negative breast cancer, when considered as a group, have a worse outcome after chemotherapy than patients with breast cancers of other subtypes, a finding that reflects the intrinsically adverse prognosis associated with the disease.[18−20] Chemoresistance has been found in greater than 50% of patients with triple-negative breast cancer.[20] The drug resistance of triple-negative breast cancers may be altered through the use of engineered systems that can increase intracellular drug concentrations overwhelming certain resistance mechanisms.[3,20,21]

Here, we have engineered biodegradable nanoparticles that improve the therapeutic index of docetaxel by altering the pharmacokinetic profile of the drug with the goal of treating taxane-resistant triple-negative breast cancer. The *in vivo* performance of PLGA-docetaxel nanoparticles, including pharmacokinetic (PK) profiles, efficacy, and tolerability, was tested in multiple cancer models, showing significant improvement over the clinical formulation of docetaxel. Nanotechnology-enabled delivery of docetaxel is a promising strategy for the treatment of triple-negative breast cancer.

Rod-shaped PLGA-docetaxel nanoparticles fabricated using the PRINT technology had a hydrodynamic diameter of 215.2 ± 2.1 nm and polydispersity index values of 0.05 ± 0.01 nm with a zeta-potential of −2.9 ± 0.2 mV, as measured by dynamic light scattering and zeta potential instruments. Analysis of the particles by scanning electron microscopy (SEM) verified that the PLGA-docetaxel nanoparticles were of defined size and shape (Figure 1A). Drug loading of the PLGA-docetaxel nanoparticles was 39.1 ± 3.9%, as determined over ten separate batches.

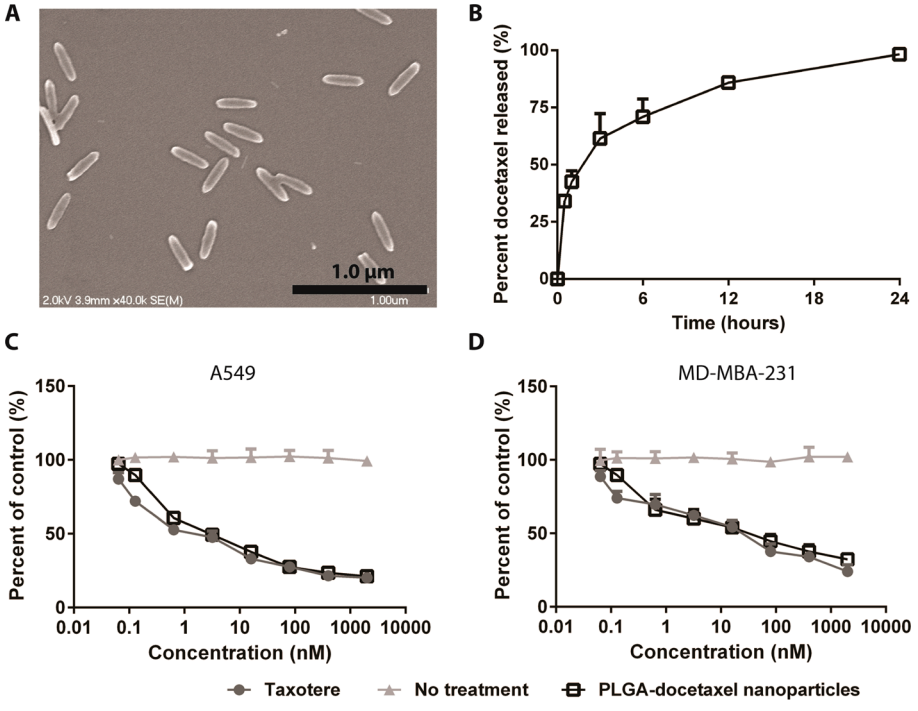

Figure 1. PLGA-docetaxel nanoparticles used to improve the therapeutic index of docetaxel. (A) SEM image of rod-shaped PLGA-docetaxel nanoparticles. (B) Release kinetics of docetaxel from PLGA-docetaxel nanoparticles in PBS at 37 °C. Cytotoxicity of Taxotere and PLGA-docetaxel nanoparticles were assessed in (C) A549 and (D) MD-MBA-231 cells. Data are means ± standard deviations (SD).

DOI: 10.1021/acs.nanolett.6b03971
Nano Lett. XXXX, XXX, XXX−XXX

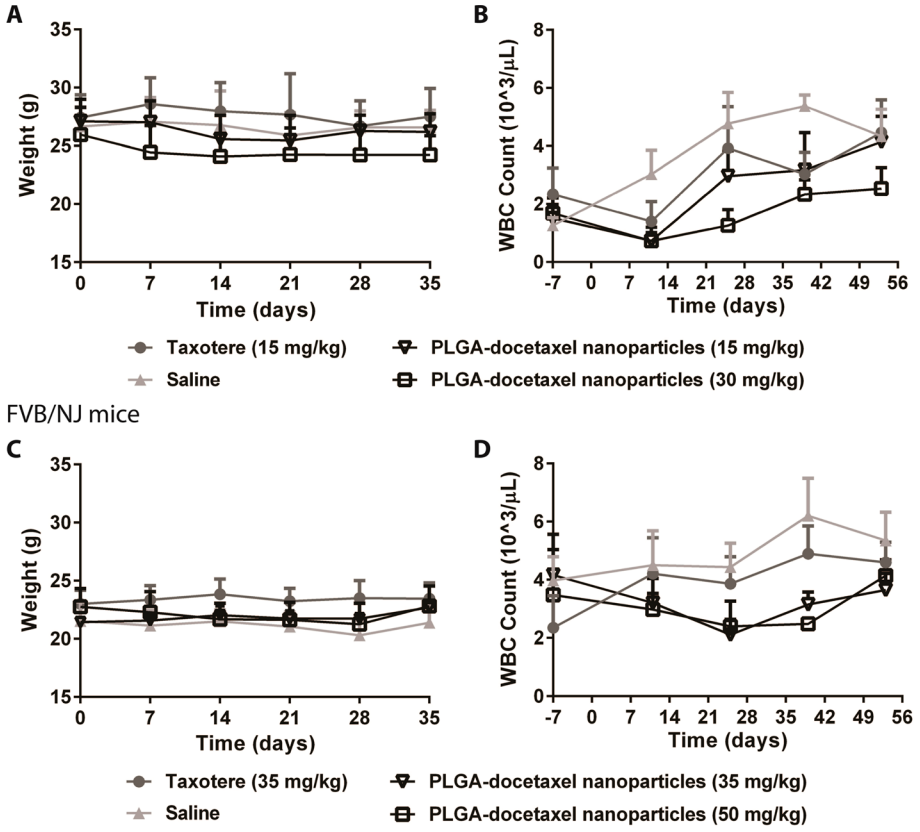

Figure 2. MTD of Taxotere and PLGA-docetaxel nanoparticles was evaluated in nontumor-bearing mice. (A) Weight and (B) WBC counts were evaluated in nude mice after five weekly injections of saline, Taxotere, or PLGA-docetaxel nanoparticles. In addition, (C) weight and (D) WBC counts were evaluated in FVB/NJ mice after five weekly injections of saline, Taxotere, and PLGA-docetaxel nanoparticles. Data are means ± SD (n = 8 animals per group).

The release rate of docetaxel from the PLGA-docetaxel nanoparticles was determined to be up to 100% at 24 h (Figure 1B).

The in vitro cytotoxicity of PLGA-docetaxel nanoparticles was tested against two cell lines, A549 and MD-MBA-231 cells. The A549 cell line was chosen because it can be directly established as a subcutaneous xenograft in nude mice and had been previously investigated.[15] The MD-MBA-231 cell line was chosen because of the same K-Ras and P53 mutations that are represented in the C3Tag GEMM. PLGA-docetaxel nanoparticles had equivalent cytotoxicity against the A549 cell line (IC_{50} 3.1 nM) when compared to Taxotere (IC_{50} 2.3 nM) (Figure 1C). In the MD-MBA-231 cell line, PLGA-docetaxel nanoparticles had similar cytotoxicity (IC_{50} 53.2 nM) to Taxotere (IC_{50} 63.4 nM) (Figure 1D).

Dosing of the PLGA-docetaxel nanoparticles was then evaluated in nontumor-bearing female nude and FVB/NJ mice. Major dose limiting toxicities of docetaxel were determined by a reduction in white blood cell count (WBC), body weights, and body composition scores. The maximum tolerated dose (MTD) for weekly dosing of Taxotere in nude mice, as previously studied, was observed to be 15 mg/kg for Taxotere.[15] PLGA-docetaxel nanoparticles dosed at 15 and 30 mg/kg docetaxel showed no loss in body weight or neutropenia in nude mice (Figure 2A,B). PLGA-docetaxel nanoparticles dosed at 35 mg/kg resulted in significant body weight loss (>20%) in two of five mice and required euthanasia. For FVB/NJ mice, the MTD for weekly dosing of Taxotere was 35 mg/kg.[15] PLGA-docetaxel nanoparticles were dosed at 35 and 50 mg/kg docetaxel in FVB/NJ mice, with no adverse events or dose-limiting toxicities after a course of five weekly doses (Figure 2C,D). Three of five mice dosed with 55 mg/kg of PLGA-docetaxel nanoparticle doses exhibited significant toxicity that required euthanasia.

Pharmacokinetic and biodistribution studies demonstrated that PLGA-docetaxel nanoparticles increased docetaxel plasma area under the concentration (AUC) curve and circulation half-life ($T_{1/2}$) and had similar tumor accumulation compared to Taxotere in A549 xenografts (Table 1, Figure 3A,B). One caveat to the calculated AUC is that the concentration at t = 5 min was used, which is a time point where more unencapsulated drug would have left the circulation compared to encapsulated drug. A single time-point analysis was performed in the C3Tag GEMMs to determine docetaxel accumulation in tumor and plasma for PLGA-docetaxel nanoparticles compared to Taxotere at 6 h postinjection (Figure 3C,D). The administration of PLGA-docetaxel nanoparticles resulted in a 376-fold increase in docetaxel plasma concentration compared to Taxotere (32.525 ± 13.703 versus 0.0865 ± 0.0078 μg docetaxel/mL plasma) (Figure 3C). In addition, delivery of PLGA-docetaxel nanoparticles led to an approximate 2-fold nonsignificant increase in tumor accumulation compared to Taxotere (9.766 ± 7.733 versus 5.729 ± 1.668 μg docetaxel/g tissue) (Figure 3D). Overall, PLGA-docetaxel nanoparticles increased docetaxel exposure in plasma and provided similar docetaxel exposure in tumor compared to Taxotere.

Overall survival and tumor growth inhibition were used as metrics to determine efficacy. Studies in A549 xenografts were performed to validate efficacy of PLGA-docetaxel nanoparticles.

DOI: 10.1021/acs.nanolett.6b03971
Nano Lett. XXXX, XXX, XXX−XXX

Table 1. PK of Docetaxel Delivered through PLGA-Docetaxel Nanoparticles and Taxotere in A549 Xenografts[a]

specimen	parameter	units	formulation: Taxotere	formulation: PLGA-docetaxel nanoparticles
plasma	$AUC_{0-\infty}$	μg/mL·h	1,227 (0−72 h)	79.192 (0−72 h)
	CL	mL/h/kg	8.150	0.126
	Vd	mL/kg	10.508	4.513
tumor	AUC_{0-t}	μg/mL·h	73.222 (0−72 h)	60.858 (0−72 h)
	C_{max}	μg/mL	0.453	0.476
	C_{last}	μg/mL	0.142	0.117
	T_{last}	h	72	72

[a]Mice were administered a single treatment of Taxotere or PLGA-docetaxel nanoparticles. Organs were collected from each animal at various times, and total docetaxel concentrations were analyzed. Data are means ± SD (n = 3 to 5 animals per group). The limit of docetaxel quantitation was 1 ng/mL.

Mice with subcutaneous A549 tumors were treated once per week for up to 6 weeks with saline, Taxotere (15 mg/kg), and PLGA-docetaxel nanoparticles (30 mg/kg) (Figure 4A). PLGA-docetaxel nanoparticles improved tumor growth inhibition compared to saline and Taxotere (Figure 4B); however, the differences were not statistically significant. Mice treated with PLGA-docetaxel nanoparticles had a significantly longer median overall survival time (>115 days) than saline and Taxotere (23 and 41 days, respectively) (Figure 4C).

Subsequently, efficacy of PLGA-docetaxel nanoparticles was evaluated in C3Tag GEMM. As C3Tag GEMMs develop multiple tumors, tumor growth for each mouse was determined as the sum of all tumor volumes versus time; also, the threshold to reach tumor burden decreased as total number of tumors increased. Mice were treated once per week for up to 6 weeks with saline, Taxotere (35 mg/kg), or PLGA-docetaxel nanoparticles (50 mg/kg) (Figure 4A). At day 18, mice treated with PLGA-docetaxel nanoparticles and Taxotere developed significantly less tumors than mice treated with saline (Figure 4D). Mice treated with PLGA-docetaxel nanoparticles showed a significant improvement in tumor growth inhibition compared to mice treated with saline, but no statistical difference was noted between the two docetaxel treatments (Figure 4E). At day 20, 83% of mice treated with Taxotere and 67% of mice treated with saline had reached tumor burden compared to 0% of mice treated with PLGA-docetaxel nanoparticles (Figure 4F). Mice treated with Taxotere and saline had similar median survival times of 20 and 19 days, respectively, which was significantly shorter than the median survival time for mice treated with PLGA-docetaxel nanoparticles (45 days). Overall, PLGA-docetaxel nanoparticles improved survival and tumor growth inhibition compared to Taxotere in the C3Tag GEMM.

Here, we demonstrated that PLGA-docetaxel nanoparticles can deliver substantial amounts of docetaxel to tumors. The nanoparticle treatment significantly improved tumor growth inhibition and survival in a taxane-resistant triple-negative breast cancer GEMM using a higher dose of the well-tolerated encapsulated drug. Genetically engineered mouse models have proven to be excellent models for recapitulating the genetics and heterogeneity of human tumors and highly predictive of the responsiveness to drug therapy.[22,23] Our preclinical results suggest that nanoparticle delivery of docetaxel may potentiate

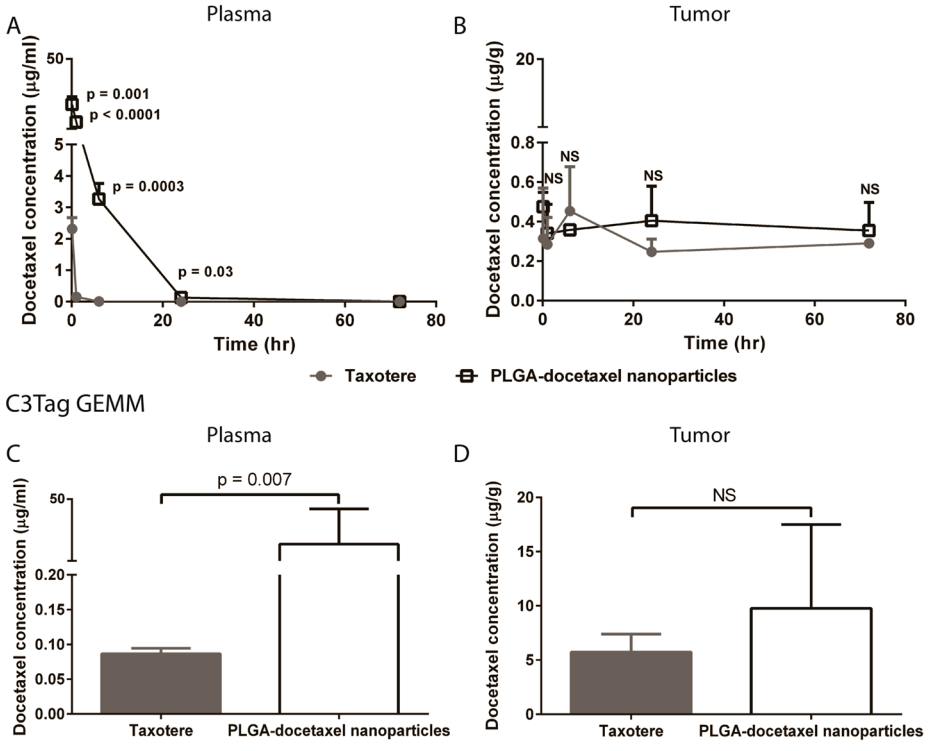

Figure 3. PK data for Taxotere and PLGA-docetaxel nanoparticles in A549 xenografts and C3Tag GEMMs. (A) Plasma and (B) tumor exposure in A549 xenograft mice after a single tail vein injection of Taxotere or PLGA-docetaxel nanoparticles. (C) Plasma and (D) tumor exposure in C3Tag GEMMs 6 h after a single tail vein injection of Taxotere or PLGA-docetaxel nanoparticles. Data are means ± SD (n = 3 to 5 animals per group). P values were determined by one-way ANOVA with unpaired t test comparing Taxotere and PLGA-docetaxel nanoparticles.

DOI: 10.1021/acs.nanolett.6b03971
Nano Lett. XXXX, XXX, XXX−XXX

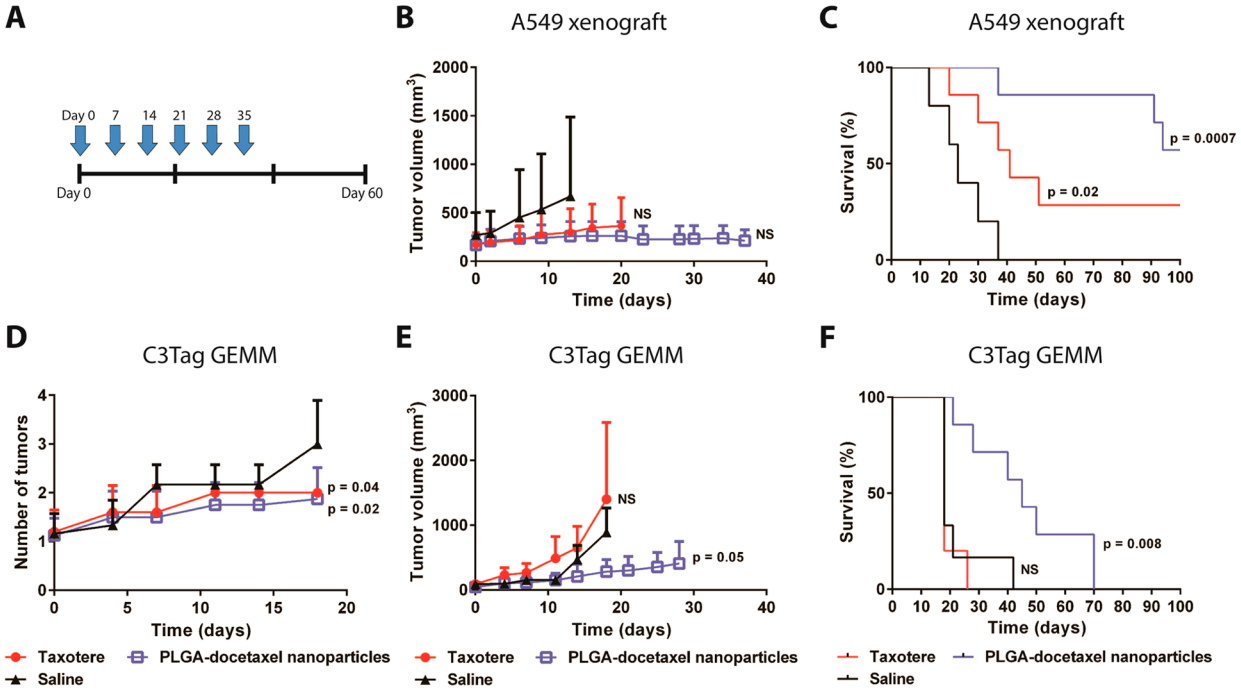

Figure 4. Efficacy of PLGA-docetaxel nanoparticles in A549 xenografts and C3Tag GEMM. (A) Treatment schedule for efficacy studies. Evaluation of (B) tumor growth inhibition and (C) survival in A549 xenografts. (D) Number of tumors, (E) tumor growth inhibition, and (F) survival were assessed in C3Tag GEMM. Data are means ± SD (n = 6–9 per group). P values were determined by one-way ANOVA with unpaired t test comparing number of tumors. P values were determined by log rank tests for comparing survival.

the current treatment of triple-negative breast cancer by enhancing the drug's therapeutic index. Moreover, this therapy could be used in combination with other therapies. One tremendous advantage would be to leverage the PRINT technology for delivery of multiple agents that are limited by systemic toxicity and/or drug resistance.

For patients with drug-resistant triple-negative breast cancer, nanoparticle drug delivery could provide a modality for overcoming resistance and increasing drug concentrations in tumor cells and microenvironment. The lack of known specific therapeutic targets results in a limited arsenal to treat triple-negative breast cancer, primarily consisting of standard cytotoxic chemotherapy.[24−26] In the metastatic setting, triple-negative breast cancer present with higher rates of visceral metastases has a relatively shorter medial survival of 7−13 months and has limited duration of response to successive lines of chemotherapy (median response duration of 12 weeks to first line, 9 weeks to second, and 4 weeks to third line).[26] Therefore, it is important to investigate new agents that could result in a meaningful benefit.

Looking beyond breast cancer, this platform technology can be applied to a variety of other cancers, including gastric, head and neck, nonsmall cell lung cancer, and prostate cancer. Overall, our nanoparticle therapy could potentially offer an entirely new cancer treatment.

Methods. *Materials.* Poly(D,L-lactide-*co*-glycolide) (lactide/glycolide 85:15, 0.65 dL/g inherent viscosity) (PLGA) was purchased from Sigma-Aldrich. Chloroform and solvents (acetonitrile and water) for high performance liquid chromatography (HPLC) and liquid chromatography−mass spectrometry/mass spectrometry (LC−MS/MS) were acquired from Fisher Scientific. The clinical formulation of docetaxel, Taxotere, was obtained from the University of North Carolina (UNC) at Chapel Hill hospital pharmacy. Poly(ethylene terephthalate) (PET) sheets (6″ width) were purchased from KRS plastics. Fluorocur, diameter (d) = 80 nm and height (h) = 320 nm (80 × 320 nm), prefabricated molds were provided by Liquidia Technologies.

Particle Fabrication and Characterization. PLGA-docetaxel nanoparticles were fabricated using a continuous roll-to-roll PRINT manufacturing system, as previously described.[15] Briefly, a thin film of PLGA and docetaxel was drawn on a 6″ × 12″ sheet of PET by spreading 150 μL of a PLGA-docetaxel-chloroform (10 mg/mL PLGA and 10 mg/mL docetaxel) solution using a #5 Mayer Rod (R.D. Specialties). The chloroform was evaporated using a heat gun. The PLGA-docetaxel film was then placed in contact with the patterned side of a mold containing 80 × 320 nm cavities and then passed through a heated laminator at 130 °C and 80 PSI to fill the cavities with polymer and drug. The mold was split from the PET sheet as they passed through the heated laminator. The filled side of the mold was then placed in contact with a sheet of PET coated with 2000 g/mol poly(vinyl alcohol) (PVOH) and passed through the heated laminator to transfer the particles from the mold to the PVOH-coated PET sheet. The PVOH was used as a transfer layer to generate a particle suspension after dissolving the PVOH with water. Subsequently, the mold was peeled from the PET sheet, and the particles were removed by passing the PVOH-coated PET sheet through motorized rollers and applying water to create a particle suspension. The particle suspension underwent tangential flow filtration (Spectrum Laboratories) to remove excess PVOH, and the particle suspension was then freeze-dried (Labconco). Nanoparticle size and zeta potential were determined by Malvern Instruments Zetasizer, and size and shape were confirmed by a Hitachi model 2−4700 SEM. Particle concentration was determined using thermogravimetric analysis correcting for the supernatant (TA Instruments). Drug loadings were quantified by dissolving the PLGA-docetaxel nanoparticles and analyzing solutions by ultraviolet spectroscopy−HPLC. For drug release

DOI: 10.1021/acs.nanolett.6b03971
Nano Lett. XXXX, XXX, XXX−XXX

studies, particle solutions were placed in mini-dialysis units with 20 kDa molecular weight cutoff and dialyzed again 1 × PBS at 37 °C. To determine the percent of docetaxel released over time, the amount of docetaxel remaining was compared to the initial amount of docetaxel in the system.

In Vitro Cytotoxicity. A549 and MD-MBA-231 cells were purchased directly from the American Type Culture Collection prior to initiation of these studies. All cell-based assays were performed utilizing cells at passage numbers ranging from 6 to 16. A549 and MD-MBA-231 cells were seeded in 200 μL of media (RPI 1640 or Leibovitz's L-15 medium (respectively) with 10% fetal bovine serum) at a density of 5000 cells per cm^2 into a 96-well microtiter plate. Cells were allowed to adhere for 24 h and then incubated with PLGA-docetaxel nanoparticles and Taxotere at docetaxel concentrations ranging from 4 μM to 0.05 nM for 72 h at 37 °C in a humidified 5% CO_2 atm. After the incubation period, all medium/nanoparticles were aspirated off cells. One hundred microliters of fresh medium was added back to cells followed by the addition of 100 μL of CellTiter-Glo Luminescent Cell Viability Assay reagent. Plates were placed on a microplate shaker for 2 min (min), then incubated at room temperature for 10 min to stabilize luminescent signal. The luminescent signal was recorded on a SpectraMax M5 plate reader. The viability of the cells exposed to PLGA-docetaxel nanoparticles was expressed as a percentage of the viability of untreated cells.

Animal Studies. All in vivo studies were approved by the Institutional Animal Care and Use Committee (IACUC) and were in accordance with The Guide for Care and Use of Laboratory Animals, eighth edition. For the A549 human tumor xenografts, athymic nude-FoxN1nu female mice were bred in-house by the UNC Animal Core Facility. Tumor cells (5.0 × 106 cells in 200 μL of 1 × PBS) were injected subcutaneously into the right flank of each mouse at age 5−7 weeks. Taxane-resistant GEMMs of strain FVB/NJ carrying a transgene for C3(1)SV40 T-antigen (C3Tag) were bred in-house.[21,22] Tumor volume was calculated using the formula: tumor volume (mm^3) = ($w^2 \times l$)/2, where w = width and l = length in mm of the tumor. Mice were assessed three times weekly for signs of toxicity, including body mass and body composition. Tumors were measured twice weekly via calipers. Mice were euthanized once tumor volume approached burden as defined by UNC IACUC.

Dosing Studies. The MTD of Taxotere and PLGA-docetaxel nanoparticles for a total of five weekly doses were determined in nontumor-bearing female nude and FVB/NJ mice. Body composition scores and body masses were recorded twice weekly, and observations were made of signs of toxicity (i.e., reduced grooming, lethargy, etc.). Mice were euthanized if body mass loss equaled or exceeded 20% or if they exhibited any other signs of toxicity. Fifty microliters of blood was collected into EDTA-coated tubes by submandibular bleeding 1 week before the first injection, 4 days after the first 5 injections, and 2 weeks after the blood draw following the fifth injection. Blood was analyzed for complete blood counts with differential using a blood counter (Heska's).

PK and Biodistribution Studies. For studies in A549 xenografts, the mice were randomly assigned to the Taxotere and PLGA-docetaxel nanoparticle treatment groups (10 mg/kg docetaxel), with individual tumor volumes ranged from 40 to 253 mm^3 at the time of grouping. The dose of docetaxel administered was based upon previously published work.[15,16] Formulations were diluted to 1 mg/mL of docetaxel with normal saline and administered via a single tail vein injection. Mice (n = 3, per time point) were sacrificed at 0.083, 1, 6, 24, and 72 h after a single injection. For studies in C3Tag GEMMs, the mice (n = 5, per group) were randomly assigned to the Taxotere (35 mg/kg) and PLGA-docetaxel nanoparticle (50 mg/kg) treatment groups. Mice were sacrificed at 6 h after dosing. In both models, blood was collected via terminal cardiac puncture using K3-EDTA as an anticoagulant under CO_2 anesthesia and processed for plasma by centrifugation (1500 × g for 5 min). Plasma and tissues were placed in cryopreservation vials and preserved by snap freezing using liquid nitrogen. Tissues were stored at −80 °C until analysis by LC−MS/MS.

Docetaxel and paclitaxel stock solutions (1 mg/mL) were prepared in methanol and stored at −20 °C. The matrix for the standard curve and quality controls (QC) consisted of control mouse plasma for all plasma samples, or control tissue homogenate for the tissue being analyzed. Liver homogenate was used as a surrogate matrix for tumor samples. Docetaxel was extracted from 50 μL of standard, QC, or unknown sample by protein precipitation with 200 μL acetonitrile/0.1% formic acid containing 20 ng/mL paclitaxel internal standard. Samples were vortexed for 5 min and centrifuged at 5000 × g for 10 min at 4 °C. One hundred and fifty microliters of supernatant was transferred to a clean 1.5 mL tube, lyophilized under nitrogen, and reconstituted in 60 μL of MeOH/0.1% formic acid. Fifty microliters of sample was transferred to a silanized glass 96-well plate insert containing 50 μL of ddH2O and 10 μL of sample injected for analysis by LC−MS/MS analysis.

Efficacy Studies. A549 xenografts (n = 5−7) were randomly assigned to one of three treatment arms: saline, Taxotere (15 mg/kg), and PLGA-docetaxel nanoparticles (30 mg/kg). Once the tumor volume reached ∼150 mm^3, weekly dosing was administered for a total of six doses or until reaching tumor burden (2 cm in any dimension). Mice were euthanized at day 115 after the first therapeutic dose, if they had not yet been euthanized.

C3Tag GEMMs (n = 5−9) were randomly assigned to one of three treatment arms: saline, Taxotere (35 mg/kg), and PLGA-docetaxel nanoparticles (50 mg/kg). Once tumors reached a palpable mass of 40−64 mm^3, weekly dosing was administered for a total of six doses or until reaching tumor burden.

PK and Statistical Analyses. Data are expressed as means ± standard deviation. Graphs were created with GraphPad Prism software. Log-rank tests were used to compare survival, with analyses performed using SAS v9.3. PK parameters were assessed with PhoenixWinNonLin (version 6.0). ANOVA methods were used for comparisons of continuous values between groups. Unpaired t tests were used when an overall difference was detected. Unadjusted P values were reported for pairwise comparisons when an overall difference was detected.

AUTHOR INFORMATION

Corresponding Author

*Phone: 1-919-9622166. Fax: 1-919-9625467. E-mail: desimone@unc.edu.

ORCID

Joseph M. DeSimone: 0000-0001-9521-5095

Author Contributions

C.J.B. and J.D.B contributed equally to this work.

Funding

This work was supported by the NCI Breast SPORE program (P50-CA58223-09A1), Carolina Center for Nanotechnology

DOI: 10.1021/acs.nanolett.6b03971
Nano Lett. XXXX, XXX, XXX−XXX

Excellence (U54-CA151652 and U54-CA119343), the University Cancer Research Fund, and Liquidia Technologies, Inc.

Notes

The authors declare the following competing financial interest(s): J. M. DeSimone is a founder and maintains financial interest in Liquidia Technologies. M. E. Napier and A. N. Schorzman hold financial interest in Liquidia Technologies.

■ ACKNOWLEDGMENTS

The authors acknowledge Charlene Ross of the Animal Studies Core, Amar Kumbhar of CHANL, and Peter H. Cable of the Biomarker and Mass Spectroscopy Facility (UNC Environmental Science, and Engineering), for their support.

■ ABBREVIATIONS

PRINT, Particle Replication in Non-Wetting Templates; WBC, white blood cells; C3Tag, C3(1)-T-antigen; GEMM, genetically engineered mouse model; ICP-MS, inductively coupled plasma mass spectroscopy; AUC, area under the curve; Vd, volume of distribution; CL, clearance; C_{max}, maximum concentration; HPLC, high performance liquid chromatography; UNC, University of North Carolina; PLGA, poly(D,L-lactide-*co*-glycolide); $T_{1/2}$, circulation half-life

■ REFERENCES

(1) Gharpure, K. M.; Wu, S. Y.; Li, C.; Lopez-Berestein, G.; Sood, A. K. *Clin. Cancer Res.* **2015**, *21*, 3121−2130.
(2) Langer, R.; Weissleder, R. *JAMA* **2015**, *313*, 135−136.
(3) Wilhelm, S.; Tavares, A. J.; Dai, Q.; Ohta, S.; Audet, J.; Dvorak, H. F.; Chan, W. C. W. *Chan WCW. Nature Reviews Materials* **2016**, *1*, 16014.
(4) Von Hoff, D. D.; Mita, M. M.; Ramanathan, R. K.; Weiss, G. J.; Mita, A. C.; LoRusso, P. M.; Burris, H. A.; Hart, L. L.; Low, S. C.; Parsons, D. M.; Zale, S. E.; Summa, J. M.; Youssoufian, H.; Sachdev, J. C. *Clin. Cancer Res.* **2016**, *22*, 3157−3163.
(5) Hrkach, J.; Von Hoff, D.; Ali, M. M.; Andrianova, E.; Auer, J.; Campbell, T.; De Witt, D.; Figa, M.; Figueiredo, M.; Horhota, A.; Low, S.; McDonnell, K.; Peeke, E.; Retnarajan, B.; Sabnis, A.; Schnipper, E.; Song, J. J.; Song, Y. H.; Summa, J.; Tompsett, D.; Troiano, G.; Van Geen Hoven, T.; Wright, J.; LoRusso, P.; Kantoff, P. W.; Bander, N. H.; Sweeney, C.; Farokhzad, O. C.; Langer, R.; Zale, S. *Sci. Transl. Med.* **2012**, *4*, 128ra39.
(6) Roode, L. E.; Brighton, H.; Bo, T.; Perry, J. L.; Parrott, M. C.; Kersey, F.; Luft, J. C.; Bear, J. E.; DeSimone, J. M.; Davis, I. J. *Nanomedicine* **2016**, *12*, 1053−1062.
(7) Perry, J. L.; Kai, M. P.; Reuter, K. G.; Bowerman, C.; Christopher Luft, J.; DeSimone, J. M. *Cancer Treat. Res.* **2015**, *166*, 275−291.
(8) Kai, M. P.; Keeler, A. W.; Perry, J. L.; Reuter, K. G.; Luft, J. C.; O'Neal, S. K.; Zamboni, W. C.; DeSimone, J. M. *J. Controlled Release* **2015**, *204*, 70−77.
(9) Chu, K. S.; Finniss, M. C.; Schorzman, A. N.; Kuijer, J. L.; Luft, J. C.; Bowerman, C. J.; Napier, M. E.; Haroon, Z. A.; Zamboni, W. C.; DeSimone, J. M. *Nano Lett.* **2014**, *14*, 1472−1476.
(10) Jones, S. W.; Roberts, R. A.; Robbins, G. R.; Perry, J. L.; Kai, M. P.; Chen, K.; Bo, T.; Napier, M. E.; Ting, J. P.; Desimone, J. M.; Bear, J. E. *J. Clin. Invest.* **2013**, *123*, 3061−3073.
(11) Perry, J. L.; Herlihy, K. P.; Napier, M. E.; Desimone, J. M. *Acc. Chem. Res.* **2011**, *44*, 990−8.
(12) Gratton, S. E.; Ropp, P. A.; Pohlhaus, P. D.; Luft, J. C.; Madden, V. J.; Napier, M. E.; DeSimone, J. M. *Proc. Natl. Acad. Sci. U. S. A.* **2008**, *105*, 11613−11618.
(13) Wang, J.; Byrne, J. D.; Napier, M. E.; DeSimone, J. M. *Small* **2011**, *7*, 1919−1931.
(14) Gharpure, K. M.; Chu, K. S.; Bowerman, C. J.; Miyake, T.; Pradeep, S.; Mangala, S. L.; Han, H. D.; Rupaimoole, R.; Armaiz-Pena, G. N.; Rahhal, T. B.; Wu, S. Y.; Luft, J. C.; Napier, M. E.; Lopez-Berestein, G.; DeSimone, J. M.; Sood, A. K. *Mol. Cancer Ther.* **2014**, *13*, 1750−1757.
(15) Chu, K. S.; Schorzman, A. N.; Finniss, M. C.; Bowerman, C. J.; Peng, L.; Luft, J. C.; Madden, A. J.; Wang, A. Z.; Zamboni, W. C.; DeSimone, J. M. *Biomaterials* **2013**, *34*, 8424−8429.
(16) Chu, K. S.; Hasan, W.; Rawal, S.; Walsh, M. D.; Enlow, E. M.; Luft, J. C.; Bridges, A. S.; Kuijer, J. L.; Napier, M. E.; Zamboni, W. C.; DeSimone, J. M. *Nanomedicine* **2013**, *9*, 686−693.
(17) Reuter, K. G.; Perry, J. L.; Kim, D.; Luft, J. C.; Liu, R.; DeSimone, J. M. *Nano Lett.* **2015**, *15*, 6371−6378.
(18) Narod, S. A.; Dent, R. A.; Foulkes, W. D. *Clin. Cancer Res.* **2015**, *21*, 3813−3814.
(19) Foulkes, W. D.; Smith, I. E.; Reis-Filho, S. N. *N. Engl. J. Med.* **2010**, *363*, 1938−1948.
(20) Gluz, O.; Liedtke, C.; Gottschalk, N.; Pusztai, L.; Nitz, U.; Harbeck, N. *Ann. Oncol.* **2009**, *20*, 1913−1927.
(21) Song, G.; Darr, D. B.; Santos, C. M.; Ross, M.; Valdivia, A.; Jordan, J. L.; Midkiff, B. R.; Cohen, S.; Nikolaishvili-Feinberg, N.; Miller, C. R.; Tarrant, T. K.; Rogers, A. B.; Dudley, A. C.; Perou, C. M.; Zamboni, W. C. *Clin. Cancer Res.* **2014**, *20*, 6083−6095.
(22) Usary, J.; Zhao, W.; Darr, D.; Roberts, P. J.; Liu, M.; Balletta, L.; Karginova, O.; Jordan, J.; Combest, A.; Bridges, A.; Prat, A.; Cheang, M. C.; Herschkowitz, J. I.; Rosen, J. M.; Zamboni, W.; Sharpless, N. E.; Perou, C. M. *Clin. Cancer Res.* **2013**, *19*, 4889−4899.
(23) Sharpless, N. E.; Depinho, R. A. *Nat. Rev. Drug Discovery* **2006**, *5*, 741−754.
(24) Santa-Maria, C. A.; Gradishar, W. J. *JAMA Oncol.* **2015**, *1*, 528−534.
(25) Hudis, C. A.; Gianni, L. *Oncologist* **2011**, *16*, 1−11.
(26) Isakoff, S. J. *Cancer J.* **2010**, *16*, 53−61.

DOI: 10.1021/acs.nanolett.6b03971
Nano Lett. XXXX, XXX, XXX−XXX